

# CRS-stack method for improved seismic imaging: A case study for Median Tectonic Line

\*Shohei Minato<sup>1</sup>, Takeshi Tsuji<sup>1</sup>, Toshifumi Matsuoka<sup>1</sup>, Yoshihiko Ishikawa<sup>2</sup>, Naoki Nishizaka<sup>2</sup>,  
Yuki Ohno<sup>2</sup>, Michiharu Ikeda<sup>3</sup>

<sup>1</sup>Dept. of Urban Management, Kyoto University

<sup>2</sup>Shikoku Electric Power Co. Inc.

<sup>3</sup>Shikoku Research Institute Inc.

We processed a marine multi-channel seismic (MCS) data acquired across the Median Tectonic Line (MTL) in southwest Japan using CRS-stack method. MTL is an arc-parallel strike-slip fault related to oblique subduction of the Philippine Sea plate beneath the Eurasian plate, and it separates the Ryoke belt from the Sambagawa belt throughout Southwest Japan. Because the subsurface fault geometry of the MTL have not been cleared sufficiently in seismic profiles, the high-quality seismic images are required. A common-reflection-surface (CRS) stack method is a multi-parameter stacking technique which has been proposed as an alternative to the conventional CMP-stack method. The CRS-stack method does not require the macro-velocity model and increases the stacking-fold number. Therefore the CRS-stack method has a potential to enhance reflection signals over the conventional CMP-stack method. Here we applied CRS-stack method to these low-fold seismic data acquired across the MTL and compared the results from conventional CMP-stack method. We show that the CRS-stack method enhanced the reflections signals from faults at depth as well as lithological boundaries.

## 1. INTRODUCTION

The Common Reflection Surface (CRS) stack method<sup>1)2)</sup> belongs to the macro model independent, multi parameter stacking method. In contrast to the conventional common midpoint (CMP) stack method, CRS-stack does not require explicit knowledge of macro velocity model. CRS-stack operator is characterized by the three wavefield attributes corresponding to the location, dip angle and the curvature of the local reflector segments. This is an extension of CMP-stack method which assumes horizontally layered structure and the CMP-stack operator is appeared as a special case of CRS-stack operator. CRS-stack method produces better signal to noise ratios (S/N) and better reflector continuities over the conventional CMP-stack method by increased fold and focusing curvature of local reflector segments. The CRS-stack method is successfully applied to sedimentary environment for the purpose of hydrocarbon exploration and deep seismic imaging<sup>3)</sup>.

We processed a marine multi-channel seismic (MCS) data acquired across the Median Tectonic Line (MTL) which is the most significant strike-slip fault in Japan. It is related to the Material Boundary Median Tectonic Line<sup>4)</sup> which separates the low-pressure/high-temperature

Ryoke metamorphic rocks to its north from the high-pressure/low-temperature Sambagawa metamorphic rocks to its south (Figure 1a). The western segment of the MTL is still active with a right-lateral sense of motion. Crustal structures related to the MTL have been widely investigated by the seismic reflection experiments<sup>4)5)</sup>. Although the reflection profiles from the conventional CMP-stack method show the reflection from the interface of Sambagawa metamorphic rocks, which is believed to MTL, the conventional CMP-stack has low S/N because of the low fold. We apply further the CRS-stack method and show that the CRS-stack method enhances the quality of reflection profiles over CMP-stack method.

## 2. CRS-STACK METHOD

CRS-stack method simulates a Zero-offset (ZO) section using a stacking surface operator. For the vicinity of a certain midpoint ( $x_0$ ), the amplitudes at its ZO travel time ( $t_0$ ) is simulated by using following isochron.

$$t^2(x_m, h) = \left( t_0 + \frac{2 \sin \alpha}{v_0} (x_0 - x_m) \right)^2 + \frac{2 t_0 \cos^2 \alpha}{v_0} \left( \frac{(x_m - x_0)^2}{R_N} + \frac{h^2}{R_{NIP}} \right). \quad (1)$$

This equation is a hyperbolic travel time approximation of kinematic reflection response from a curved interface described in midpoint ( $x_m$ ) and half-offset ( $h$ ) domain<sup>6</sup>). Equation 1 is a travel time from common reflection surface (CRS) which is characterized by three CRS parameter ( $\alpha$ ,  $R_N$ ,  $R_{NIP}$ ).  $\alpha$  are emergence angles of reflection rays reaching to given midpoint  $x_0$ .  $R_{NIP}$  and  $R_N$  are radii of two eigen waves called Normal wave and NIP wave respectively<sup>7</sup>). NIP wave can be explained as a wave generated from point diffraction on the CRS (Figure 2). Normal wave is generated from explosive reflector experiment of the CRS, which reaches to the vicinity of given  $x_0$ . From equation 1, one can see that the CRS-stack operator forms a surface in  $x_m$ - $h$  domain. This increases the number of traces contributing to image subsurface over the conventional CMP-stack method. Furthermore, the CRS-stack does not explicitly require the macro velocity model without surface velocity  $v_0$ . The CRS-stack method yields to a search for appropriate values of CRS parameters ( $\alpha$ ,  $R_N$ ,  $R_{NIP}$ ) for every point of ZO section. This search is based on coherency analysis<sup>8</sup>). Different combinations of CRS parameters are evaluated to search the highest coherency of signals along the CRS-stack surface in the data volume. We implemented this three dimensional parameter search as separated three one-dimensional search<sup>12</sup>). Each consists of CMP stack, Linear ZO stack, and Hyperbolic ZO stack.

The conventional CMP stack operator corresponds to the CRS stack operator by substituting  $x_m=x_0$ .

$$t^2(h) = t_0^2 + \frac{4h^2}{V_{NMO}^2}, \text{ where } V_{NMO} = \sqrt{\frac{2V_0 R_{NIP}}{t_0 \cos^2 \alpha}}. \quad (2)$$

The CMP-stack operator forms a line in  $x_m$ - $h$  domain and it only depends on a half-offset ( $h$ ) and a stacking velocity ( $V_{NMO}$ ) which is connected to the CRS parameters (equation 2). Therefore the first step of one-parameter search of CRS-stack is to search for  $V_{NMO}$  giving high coherency by testing different values of  $V_{NMO}$ . Alternatively, we can use the velocity estimated from a conventional velocity analysis. This can be utilized for the constrained CRS-stack which suppresses unwanted events such as multiple reflections<sup>3</sup>).

Linear ZO stack searches for the emergence angle ( $\alpha$ ) in the CMP stacked (ZO) section assuming linearly shaped reflectors. When the reflector has linear shapes ( $R_N=\infty$ ), the CRS stack operator in the ZO section ( $h=0$ ) can be written as,

$$t(x_m) = t_0 + \frac{2 \sin \alpha}{v_0} (x_0 - x_m) \quad (3)$$

This step is called as a Linear ZO stack. The

discretized values of  $\alpha$  are tested to find  $\alpha$  giving high-coherency in the given CMP stacked section.

Hyperbolic ZO stacks search for the radius of Normal wave (RN) with the given emergence angle. The CRS stack operator in ZO section ( $h=0$ ) is written as,

$$t^2(x_m) = \left( t_0 + \frac{2 \sin \alpha}{v_0} (x_0 - x_m) \right)^2 + \frac{2t_0 \cos^2 \alpha}{v_0} \left( \frac{(x_m - x_0)^2}{R_N} \right). \quad (4)$$

The emergence angles estimated from Linear ZO stack are used for equation 4 to find  $R_N$  giving high-coherency in the given CMP stacked section.

So-obtained CRS parameters are used for CRS-stack (equation 1). Optional optimization can be introduced on the basis of these parameters by simplex optimization method<sup>2</sup>). The CRS-stack operator is an approximation and is valid for the vicinity of the given midpoint. Therefore, the CMP aperture is an important factor for the CRS-stack. Figure3 shows the examples of the CRS-stacked section at different CMP aperture. When the CMP aperture is large (Figure3a), the lateral resolution is small by smearing. When the CMP aperture is small (Figure3b), the CRS folds do not increase dramatically and the stacked section is noisy. In practice, the CMP aperture is determined by testing the different values in our application.

### 3. DATA ACQUISITION AND PROCESSING

The study area is located in Seto inland sea between Honshu and Shikoku island (Figure 1). The survey line perpendicularly runs to the MTL with its length of 17 km (Figure 1b). The data set consists of 683 shot gathers. The interval of shot points and 48 receivers is 25m and 12.5m respectively. The maximum offset is of 662.5 m. The record length is 5.0 sec at the sampling rate of 1.0 msec. The 2777 CDP gathers provide reflection profiles. The interval of CDP is 6.25 m and the maximum CMP fold is 12

The data is first processed applying standard CMP stack scheme. We apply frequency filtering to the data set to enhance the signals. The bandpass filter (5Hz to 50 Hz) is applied. The main frequency of the data set is 25Hz. We apply AGC (gate length is 1.5 sec) to recover the amplitude. The data set contain many multiple reflections. Therefore, after CMP sorting each CMP gather is transformed into  $\tau$ - $p$  domain and a prediction error filter is applied to suppress the multiple reflections. Finally the data is inverse-transformed into space-time domain.

The conventional CMP stacked section after

migration is shown in Figure 4. The velocity analysis is performed at every 1km and the interpolated velocity structure ( $V_{NMO}$ ) is used to produce the images of subsurface structures. The CMP stacked section shows the horizontally-layered Neogene-Quaternary sediments (Figure 4). The steeply dipping reflector between CMP2200 and CMP2700 is the top of the Sambagawa metamorphic rocks (material boundary MTL). The irregular shaped boundary which is recognized around TWT 1 sec to 2 sec between CMP1 and CMP1400 is the top of the Ryoke granitic rocks.

#### 4. IMPROVED IMAGE BY CRS-STACK

The conventional CMP-stack produced the reflection profile where the reflection boundaries can be recognized, however, the small number of CMP folds (maximum is 12) causes low S/N. Furthermore, the remaining multiple reflections contaminate reflection signals. Therefore it is difficult to track the boundaries at depth. We apply CRS-stack method to improve these reflection profiles.

In order to estimate appropriate values of CRS parameters ( $\alpha$ ,  $R_N$ ,  $R_{NIP}$ ), the different combination of CRS parameters are tested. First, we apply the Linear ZO-stack (equation 3) to estimate emergence angles ( $\alpha$ ). We apply AGC (gate length of 500msec) to the CMP-stacked section and use the image for the Linear ZO stack. Secondly, we conduct the Hyperbolic ZO stack (equation 4) to estimate radius of Normal wave ( $R_N$ ) based on the  $\alpha$  searched from the Linear ZO stack. The CMP aperture is set to 50 m at 0.75 sec and 200 m at 2 sec, which is linearly interpolated. Finally we transformed  $V_{NMO}$  to the radius of NIP wave ( $R_{NIP}$ ) by equation 2. We get CRS parameters and apply the CRS-stack and migration (Figure 5). The CRS stacked section has higher S/N over the CMP stacked section (Figure 4). The lateral continuity of the sediments is enhanced. Furthermore, the boundary of the Ryoke granitic rocks and Sambagawa metamorphic rocks, which is the MTL on the CRS-stack image, is clearer than the CMP stacked section. However, the structural relationship between active faults and the geological boundary fault is not sufficiently cleared on the CMP/CRS stacked sections. The point is one of the intriguing and important targets to be cleared in the future.

#### 5. CONCLUSION

We applied the CRS-stack method to marine multi channel seismic (MCS) data acquired across

the Median Tectonic Line (MTL) of southwest Japan. The reflection profile from the conventional CMP-stack method shows the boundary of Sambagawa metamorphic rocks and the boundary of Ryoke granitic rocks, which is imaged up to TWT 2.5 sec. However mainly because of the low CMP folds, the reflection profile is low S/N and it is difficult to track these boundaries. The CRS-stack method enhanced S/N of the reflection profiles over the CMP-stack method and also enhanced the reflector continuity of the Sambagawa metamorphic rocks and the Ryoke granitic rocks.

#### REFERENCES

- 1) Mann, J.; Jäger, R.; Müller, T.; Höcht, G. and Hubral, P., 1999, Common-reflection-surface stack--A real data example, *Journal of Applied Geophysics* **42**(3-4), 301-318.
- 2) Jäger, R.; Mann, J.; Höcht, G. and Hubral, P., 2001, Common-reflection-surface stack: Image and attributes, *Geophysics* **66**(1), 97-109.
- 3) Yoon, M.; Baykulov, M.; Dümmling, S.; Brink, H. and Gajewski, D., 2009, Reprocessing of deep seismic reflection data from the North German Basin with the Common Reflection Surface stack, *Tectonophysics* **472**(1-4), 273-283.
- 4) Ito, T.; Ikawa, T.; Yamakita, S. and Maeda, T., 1996, Gently north-dipping Median Tectonic Line (MTL) revealed by recent seismic reflection studies, southwest Japan, *Tectonophysics* **264**(1-4), 51-63.
- 5) Kawamura, T.; Onishi, M.; Kurashimo, E.; Ikawa, T. and Ito, T., 2003, 'Deep seismic reflection experiment using a dense receiver and sparse shot technique for imaging the deep structure of the Median Tectonic Line (MTL) in east Shikoku, Japan', *Earth, planets and space* **55**(9), 549-557.
- 6) Höcht, G.; de Bazelaire, E.; Majer, P. & Hubral, P., 1999, Seismics and optics: hyperbolae and curvatures, *Journal of Applied Geophysics* **42**(3-4), 261-281.
- 7) Hubral, P., 1983, Computing true amplitude reflections in a laterally inhomogeneous earth, *Geophysics* **48**(8), 1051-1062
- 8) Neidell, N. S. and Taner, M. T., 1971, SEMBLANCE AND OTHER COHERENCY MEASURES FOR MULTICHANNEL DATA, *Geophysics* **36**(3), 482-497.
- 9) Wallis, S., 1998, Exhuming the Sanbagawa metamorphic belt: the importance of tectonic discontinuities., *Journal of Metamorphic Geology* **16**(1), 83

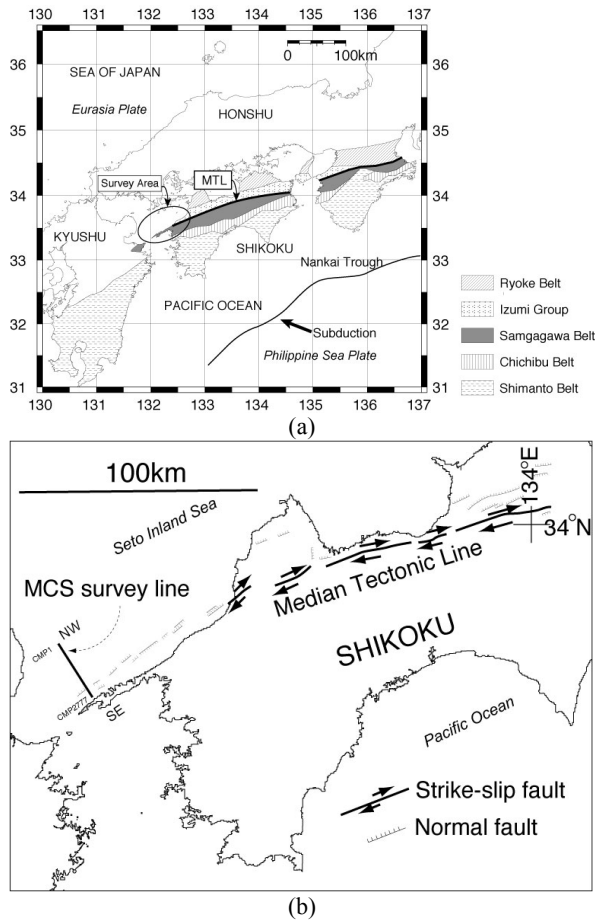


**Figure 1:** (a) Index map showing tectonic map of Southwest Japan<sup>9)</sup>. (b) Strike-slip fault and normal fault around our seismic line.

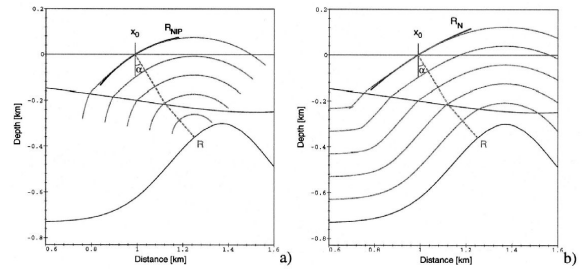


**Figure 2:** Schematic figure of eigen wave and CRS parameter (from Jäger et al., 2001)

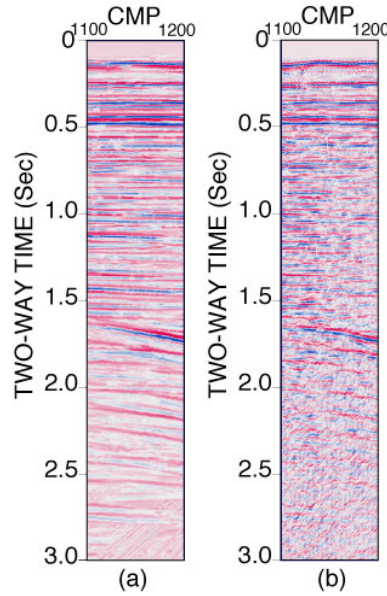


**Figure 3:** CRS stacked section at CMP 1100-1200 from our data with different CMP aperture. (a) CMP aperture of 500m. (b) CMP aperture of 10m. The result of small CMP aperture is contaminated by noise and the result of large CMP aperture is small lateral resolution.

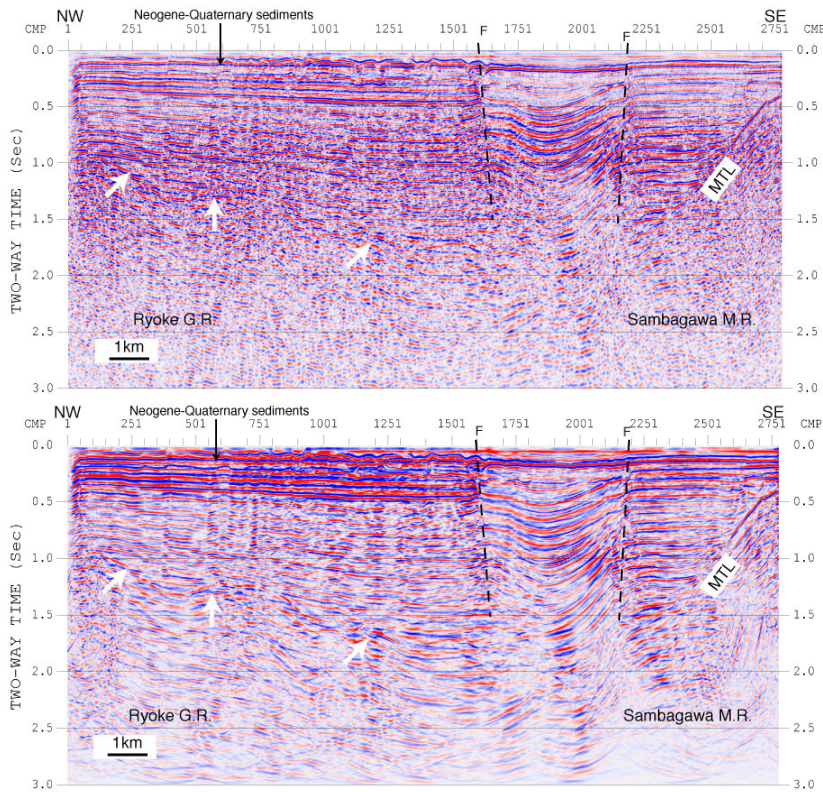


**Figure 4:** Migrated CMP section. The horizontal layered structure shows sediment rocks. North dipping reflector between CMP2200 and CMP2700 is a top of Sambagawa metamorphic rocks (MTL). The arrows show the irregular shaped boundary of Ryoke granitic rocks. Dashed lines are interpreted active faults.

**Figure 5:** Migrated CRS section. S/N and the reflector continuity of the sediments, the boundary of Sambagawa metamorphic rocks, and the Ryoke granitic rocks are significantly improved over CMP-stack (compare with Figure 4).